Sub-monolayer growth of Ag on flat and nanorippled SiO_2 surfaces

Mukul Bhatnagar,[1,2] Mukesh Ranjan,[1,2] Kenny Jolley,[3] Roger Smith,[3] and Subroto Mukherjee[1,2]
[1)] *FCIPT, Institute for Plasma Research, Gandhinagar 382428, Gujarat, India*
[2)] *Nirma University, Ahmedabad 382481, Gujarat, India*
[3)] *Dept. of Mathematical Sciences, Loughborough University, Leicestershire, LE11 3TU, UK*

In-situ Rutherford Backscattering Spectrometry (RBS) and Molecular Dynamics (MD) simulations have been used to investigate the growth dynamics of silver on a flat and the rippled silica surface. The calculated sticking coefficient of silver over a range of incidence angles shows a similar behaviour to the experimental results for an average surface binding energy of a silver adatom of 0.2 eV. This value was used to parameterise the MD model of the cumulative deposition of silver in order to understand the growth mechanisms. Both the model and the RBS results show marginal difference between the atomic concentration of silver on the flat and the rippled silica surface, for the same growth conditions. For oblique incidence, cluster growth occurs mainly on the leading edge of the rippled structure.

Silver nanoparticles have widespread application in nanotechnology and are being used in diverse applications ranging from bio nanoscience[1], thermal applications[2] and photovoltaics[3,4]. Our interest arises from their optical properties due to the interaction of the conduction electron cloud of a nanoparticle with incident electromagnetic radiation. This characteristic optical signature known as Localised Surface Plasmon Resonance has been a well studied topic[5]. However, the growth of metallic nanoparticles on flat oxidised surfaces is not yet fully understood. For some surfaces and growth conditions, there is a Volmer Weber mode that leads to the formation of separated clusters until the thickness of the film reaches around 100 nm[6]. However layer by layer growth can also occur, e.g. on ZnO[7]. Recently, studies were undertaken using lattice-based Kinetic Monte Carlo (KMC) to model the growth of Ag nanoparticles on a rippled SiO_2 surface[8]. The model used simplified assumptions such as no reflection of Ag, no cluster migration and no energy nor angle of incidence dependence of the incident Ag[8,9]. In addition the underlying lattice was assumed to be face-centred cubic (fcc) so it was not clear if the predicted growth patterns were affected by this. Here, we perform in-situ RBS to measure the dependency of atomic concentration on the angle of incident (AOI) of the silver flux for the flat SiO_2 surface and compare it with a rippled silica surface. We use MD to understand the dependency of the sticking coefficient on the binding energy (E_b) of the silver to the surface and the kinetic energy (K.E.) of the incident Ag for multiple AOIs. A potential parameterisation using the optimum value of E_b is then used in the simulation to deposit silver successively.

The modification of a crystalline silicon surface to a rippled structure is a well studied topic[10,11]. We report in brief the fabrication process of a ripple pattern on silicon and the subsequent deposition of silver on the flat and the rippled surface. An epi-polised silicon wafer (100) was bombarded by a 500 eV broad beam of Ar^+ ions at an AOI = 67° to the surface normal. The generated rippled silicon (periodicity ≈ 35 nm, amplitude ≈ 2 nm) has an asymmetric nature where two planar surfaces subtend different angles to the average surface normal (see Fig. 1, image (d)). This substrate was then exposed to atmosphere which leads to the formation of a native oxide layer on the surface. Subsequent deposition of silver was performed using an electron beam evaporation system at a pressure of 10^{-8} mbar. The PVD system is mounted directly on the RBS beam line for performing in-situ measurements to monitor the growth of silver clusters on both the flat silica surface and rippled silica surface simultaneously. The deposition rate was tuned through RBS and fixed at 0.1 ML/min, where 1 ML for a fcc silver lattice corresponds to the surface density of 1.2x10^{15} atoms/cm^2. The direction of the incident vapour flux was varied from 0° to 85° to the surface normal. The RBS beam line generates an incident beam of He^{2+} ions with kinetic energy 1.7 MeV. The system uses a geometry[12], where the incident angle of the He^{2+} ions is 40°; the exit angle is 50° and scattering angle is 170°. The raw RBS data was fitted using the SIMNRA[12] software to extract the atomic density of the silver present on the silica surface at a constant time interval of one minute. The deposition of silver and the in-situ RBS measurements were done at room temperature.

We prepared a special sample (1 cm^2) which was partly flat and partly rippled (Fig 1, image (b)). Plot (a) of fig. 1 shows the distribution of the incident atomic flux from the evaporator onto this substrate. It is seen that the incident flux is constant for a width of 14 mm. Image (b) shows the topology of both the flat surface and the rippled surface with a schematic of the points of measurement for in-situ RBS. A separation of 5 mm was kept to avoid variation of deposited silver over the measurement region. All our experimental results are from the deposition of silver on this substrate as this makes the RBS measurements independent of the deviation of the atomic flux in the two different regions. Image (c) and image (d) show the SEM images of the deposited silver at an AOI of 70°. It is clearly visible from both the images that the deposited silver nanoparticles grow by the Volmer Weber mode[13] and in the case of the rippled surface, silver nanoparticles follow the topology of the underlying template as previously observed[6,14].

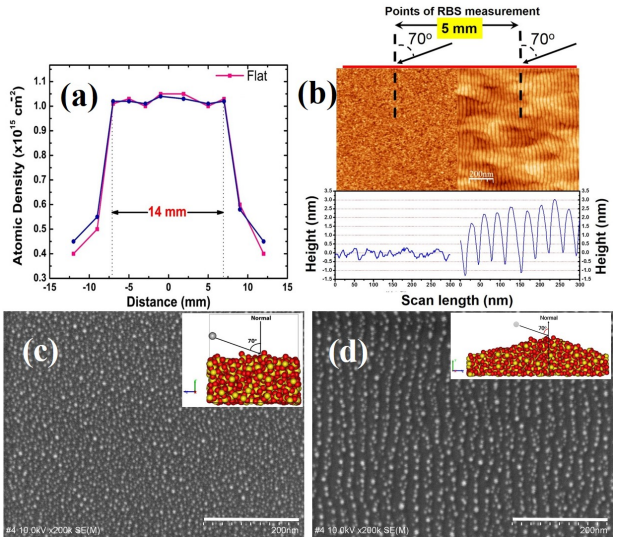

FIG. 1. (Colour online) (a): RBS measurement of atomic flux over a width of 14 mm on a partly flat and partly rippled surface. (b): Images showing the sites for RBS measurements. The angle of incidence was kept fixed at 70° to the average surface normal. Atomic force microscope (AFM) analysis of the two substrates show that the RMS surface roughness for the flat surface is ≈ 0.2 nm whereas the amplitude modulation on the rippled surface is ≈ 2 nm. Images (c) and (d) show scanning electron micrographs (SEM) after cross deposition of silver. The inset in image (c) shows the direction of the incidence Ag atoms. The inset in image (d) shows the deposition geometry on the rippled surface. The red spheres correspond to the oxygen atoms and the yellow spheres silicon.

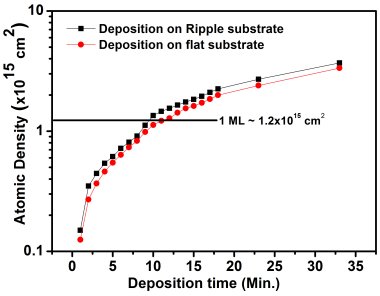

FIG. 2. (Colour online) Plot shows the atomic concentration of the silver on the flat and the rippled silica surface obtained through in-situ RBS. The angle of deposition was kept fixed at 70° w.r.t the surface normal of the flat silica surface.

Fig. 2 shows a comparison of the observed atomic density of silver on the flat silica surface and the rippled silica surface for an AOI = 70°. It is seen that there is minimal difference in the atomic concentration of silver on both the surfaces. A similar trend was observed in several such experiments. Since the growth was performed only up to the equivalent of a few monolayers, the atomic density does not show any saturation before the completion of the experiment.

To understand the results obtained from RBS measurements, we used MD[15] to simulate the interaction of a silver atom with the silica surface. The detailed description of the potentials used in this work is given in the supplementary material S1[16]. Since there is a lack of experimental or ab initio data that gives a value for the average binding energy of Ag to SiO_2, we fit a simple pairwise Morse potential for the Ag-Si and Ag-O interactions. We chose two sets of parameters that gave average binding energies of 0.2 and 0.6 eV. The former value is consistent with previous lattice-based KMC simulations[8].

Initially, 800 independent impact events (incident Ag atom energy, $E_{Ag} = 1.0\,eV$) were performed on a rectangular silica substrate. The procedure to create an amorphous silica surface was as follows: A charge neutral SiO_2 substrate was generated with random positions of silicon and oxygen atoms. A total of 999 atoms was chosen so as to create a big enough surface to simulate the silver-silica interaction. The simulation box was generated by calculating the volume of the box required to hold 333 atoms of silicon and 666 atoms of oxygen with the density of silica taken as 2.65 g/cm^3. The dimensions of the box were X = 2.92 nm, Y = 1.46 nm and Z = 2.92 nm and initially periodic boundary conditions (PBC) in all cartesian directions were used. The structure was then relaxed using a quench process[17] until the system temperature was below 100K. The system was finally minimised using damped MD to remove excess energy. To create a free surface for SiO_2, the box size was increased in the Y direction to 2.92 nm. The bottom 3 layers of the solid were kept fixed so as to avoid wrapping the lowest layer of atoms with the top of the vacuum region above the SiO_2 surface. As the atoms present on the surface need to be relaxed within the new box size (X = 2.92 nm, Y = 2.92 nm and Z = 2.92 nm), the system was damped again for t = 10 ps. Thus the average surface normal lies in the Y direction with PBC operating in the X and Z directions. The incident Ag atom was projected from a distance of 0.8 nm above the highest atom on the silica surface at different incidence angles and positions to generate the data. Each impact event was carried out for a time period of 10 ps which gives enough time to decide if the Ag atom is captured by the surface. After each impact, the surface was reinitialised to be silver-free and the process repeated. Some simulations were carried out with substrates quenched from different random initial configurations.

Plot (a) of Fig. 3 shows the results obtained from the calculation of the mean sticking coefficient of silver on a flat silica surface for $E_b = 0.2\,eV$ and $E_b = 0.6\,eV$ with change in the AOI of the incident Ag atom. The surface is quite rough on the atomic scale with a maximum to minimum height variation of up to 0.8 nm, indicating that the choice of impact point could have a crucial effect on the sticking probability. As expected, plot (a) shows that the calculated sticking coefficient is less for $E_b = 0.2\,eV$ due to the shallow potential well. The sticking coefficient for $E_b = 0.6\,eV$ is high even near grazing

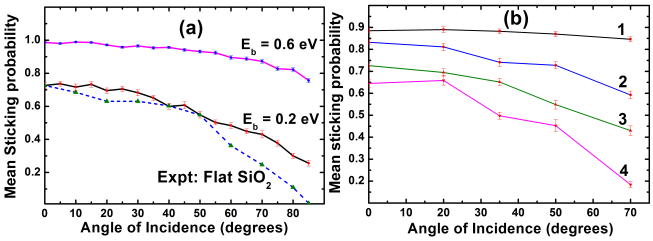

FIG. 3. (Colour online) Plot (a) shows the calculated mean sticking coefficient for silver on the flat silica surface for $E_b = 0.2\,eV$ and $E_b = 0.6\,eV$. Here $E_{Ag} = 1.0\,eV$ and T = 300 K. The RBS measurements are shown also, normalised to fit the sticking probability at normal incidence with respect to the $E_b = 0.2\,eV$ data. Plot (b) shows the variation of sticking coefficient with K.E. of the incident Ag atom. The numbers 1, 2, 3 and 4 correspond to the K.E. 0.1 eV, 0.5 eV, 1.0 eV and 2.0 eV respectively.

incidence. The experimental results show a sharper drop-off with incidence angle compared to the model. This is probably due to the model giving a rougher surface than experimentally observed. With a rough surface it might be expected that favourable sites would exist where the Ag can form more bonds with the substrate compared to a smoother surface. For the model the surface is also assumed to be stoichiometric rather than Si or O rich. In addition all impacts occur on a substrate with no added Ag, whereas in the experiment, the data is collected as the film grows. During this dynamic process, atoms can also dissociate from the surface.

The reported value of E_{Ag} for deposition through electron beam evaporation is less than 1.0 eV with a narrow energy distribution[18–20] therefore we performed a series of simulation runs at different impact energies, E_{Ag} for the same silica surface with $E_b = 0.2\,eV$. Plot (b) shows the variation of the sticking coefficient with the energy of the incident silver. It is seen that for a softer collision process ($E_{Ag} = 0.1\,eV$), the mean sticking coefficient has a small variation (4% from 0° to 70°), whereas for a harder collision ($E_{Ag} = 2.0\,eV$), the sticking coefficient is reduced by almost 70 %. The actual sticking coefficient for a partially covered surface could reduce further as events such as Ag dimer/cluster evaporation increase with the increase in E_{Ag}.

Simulation of the growth of silver on SiO_2 requires much more computing power than modelling individual atom impacts. MD simulations are limited to time scales up to microseconds at best and experimental time scales are generally not accessible by MD alone. Recently a multi-time scale technique has been developed that uses MD to model individual particle impacts over picosecond time scales followed by an off-lattice KMC approach to model diffusion between particle impacts[21]. This works well when the diffusion barriers are large so that atom movement only occurs as series of rare events. If the energy barriers for diffusion are low then the time acceleration is much more modest. We performed some simulations using this technique but found that the computed barriers were low and that Ag atoms diffused quickly to form clusters on the surface. The barriers for a single Ag to diffuse from one local minimum to another, calculated using the nudged elastic band technique[22], based on the empirical potential used to carry out the simulation, varied between 0.1 and 0.2 eV depending on the attachment site. Small clusters containing up to 4 Ag atoms were also found to be mobile on the surface over picosecond time scales. Once the larger Ag clusters were formed it was difficult for them to break apart although in some cases during a deposition event, an entire cluster could detach from the surface due to the weak bonding with the substrate. Even the deposition of a few atoms using the off-lattice KMC involved weeks of computing time. As a result we performed MD simulations at unrealistically high deposition rates for comparison. It was found that the results were qualitatively the same as using off-lattice KMC. The details of the MD simulation are as follows. We performed cumulative deposition of up to 500 silver atoms on the rippled silica surface and the flat silica surface at an AOI = 70° to the surface normal. The size of the flat silica substrate was kept as X = 5.84 nm Y = 1.56 nm and Z = 5.84 nm. The rippled silica surface was developed as follows: The quenched SiO_2 solid (X = 5.84 nm Y = 2.92 nm and Z = 5.84 nm) was cut at two different angles from the surface normal consistent with those shown in image (a) of Fig. 4. Having cut the structure, the system was relaxed using damped MD. During the relaxation, the angles of the two planes did not change greatly although there was some flattening at the top of the crest. The temperature of the substrate was kept at 300K by a heat bath of atoms located above the fixed layers in the system. The time period of each simulation was kept fixed at 20 ps which was long enough to allow for temperature equilibration and for the silver to diffuse over the surface. Each new simulation was started from a random position in the X-Z plane but at a fixed height. We used the model with $E_b = 0.2\,eV$ as the simulation results show a trend similar the reported experimental observations[23] and for comparison with the previous KMC model[9]. The choice of incident adatom K.E. ($E_{Ag} = 0.5\,eV$) was based on the fact that $E_{Ag} = 1.0\,eV$ and above is more than that observed in evaporation experiments[19] and $E_{Ag} = 0.1\,eV$ shows negligible variation of mean sticking coefficient with change in the incident angle of incidence. The evaporation rate for $E_{Ag} = 1.0\,eV$ or above is quite high when $E_b = 0.2\,eV$ and we could observe Ag clusters of up to 7 atoms being dislodged from the surface by impacting Ag.

The main growth mechanisms seen in the simulations are the diffusion of adatoms and small clusters over the surface to join existing larger clusters, the direct attachment of incoming silver atoms to a cluster and the coalescence of large clusters when they come within a certain interaction range.

Images (a) and (c) in Fig. 4 show typical results from the cumulative deposition of Ag on the rippled surface

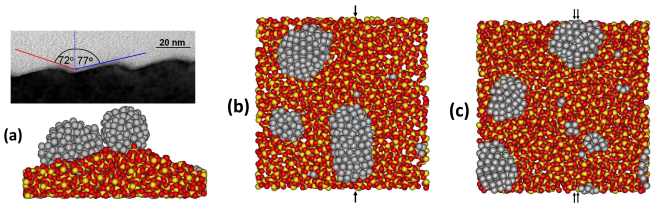

FIG. 4. (Colour online) (a): The top image shows a cross sectional Transmission Electron Micrograph of the ripple structure (periodicity ≈ 35 nm) along with the angles for the two planes of the rippled surface. The bottom image shows the side view from the simulated cumulative deposition of 500 Ag atoms on the rippled surface. (b): The corresponding top view of the rippled surface. The arrow heads mark the position of the ridge. (c): Top view of the silver deposited on the flat silica surface. The double arrows mark the position where the ridge would have appeared. The deposition parameters were $E_{Ag} = 0.5\,eV$, $E_b = 0.2\,eV$, AOI = 70° and T = 300 K.

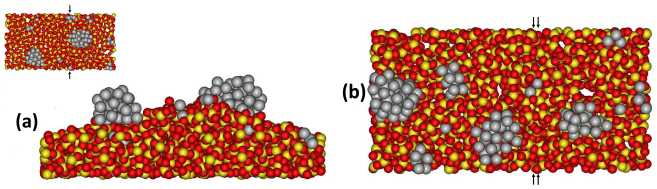

FIG. 5. (Colour online) (a): Side view of the cross deposited silver on the rippled silica surface. The inset shows the corresponding top view. (b): Top view of the deposited silver on the flat silica surface. Double arrows mark the position where the ridge would have appeard. Here the AOI = 20°. $E_{Ag} = 0.5\,eV$ and T = 300 K. Silver clusters are seen on both faces of the rippled surface and the observed growth appears similar to that on the flat surface seen in Fig. 4 for AOI = 70°.

and the flat surface at an AOI of 70°. It is seen from Fig. 4 (a) and (b), that the Ag atoms form clusters on the face of the rippled surface more exposed to the incident atomic flux. The opposite face contains less Ag. This is because at an AOI =70°, the average normal on the exposed face (A_e) makes an angle of 57° with the incident vector of the incoming Ag atom whereas the opposite face (A_o) of the rippled surface subtends an apparent angle of 88°. This leads to a decrease in the sticking coefficient for A_o. This is reflected through the plot (b) of Fig 3. which shows a change of ≈15 % in Ag coverage when the AOI changes from 57° to 70° and the difference will further increase for an AOI = 88°. The observed cluster formation on the rippled silica surface and the flat silica corresponds well with the experimental observations (Fig. 1, image (c) and image (d)) with the clusters being randomly distributed on the flat surface but with gaps on that part of the rippled surface where the incidence angle is around 88°. In addition, the rippled surface contains about 19% more silver than the flat surface for the same incidence flux. However, more runs and better statistics are required to determine if this is a repeatable observation.

Image (a) and image (b) of fig. 5 show the comparison for surface coverage of silver on the rippled silica surface and the flat silica surface for the AOI = 20°, respectively. It is seen from the final snapshots that the difference in surface coverage between the two surfaces is minimal. The model gives no Ag nanoparticle arrays for AOIs close to the surface normal, consistent with the experimental results[6].

In conclusion, the atomic density of silver is observed to be marginally different for the flat surface and the rippled surface as measured through in-situ RBS. A similar result is obtained from MD after cumulative deposition of silver for an AOI = 70°. MD simulation shows that the sticking coefficient reduces with angle of incidence for $E_b = 0.2\,eV$ in a manner consistent with the experimental results except near grazing incidence. MD was also able to identify growth mechanisms due to the low energy barriers for small Ag cluster diffusion over the surface. The cluster patterns predicted by MD are also in agreement with the observations from SEM.

The authors would like to acknowledge Ion Beam and Material Centre, HZDR, Dresden, Germany for the use of RBS facility, DST- British Council exchanges with India scheme, UKIERI Grant: IND/CONT/E/13-14/642 and the programme DST-Nanomission for funding.

[1]S.S. Aćimović, M.A. Ortega, V. Sanz, J. Berthelot, J.L. Garcia-Cordero, J. Renger, S.J. Maerkl, M.P. Kreuzer and R. Quidant, Nano Lett. **14**, 2636 (2014).
[2]S. Link and M. A. El-Sayed, Int. Rev. Phys. Chem. **19**, 409 (2000).
[3]U. W. Paetzold, E. Moulin, B.E. Pieters, R. Carius and U. Rau, Opt. Express **19**, A1219 (2011).
[4]H. Tan, L. Sivec, B. Yan, R Santbergen, M. Zeman and A.H. Smets, Appl. Phy. Lett. **102**, 153902 (2013).
[5]S. A. Maier, Plasmonics: fundamentals and applications, Springer, (2007).
[6]M. Ranjan, S. Numazawa and S. Mukherjee, Mater. Res. Express. **1**, 015038 (2014).
[7]S. Blackwell, R. Smith, S. D. Kenny, J.M. Walls and C.F. Sanz-Navarro, J. Phys. Cond. Matt **25**, 135002 (2013).
[8]S. Numazawa, M. Ranjan, K. H. Heinig, S. Facsko and R. Smith, J. Phys. Cond. Matt **23**, 222203 (2011).
[9]S. Numazawa and R. Smith, Phy. Rev. E **84**, 046714 (2011).
[10]M Ranjan, Journal of nanoparticle research 15.9: 1-10, (2013).
[11]A. Keller, S. Facsko and W. Möller, J. Phys. Cond. Matt **21**, 495305 (2009).
[12]M. Mayer, Proc. The fifteenth international conference on the application of accelerators in research and industry. 475, (1999).
[13]M Lončarić, J. Sancho-Parramon, M. Pavlović, H. Zorc, P. Dubček, A. Turković, S. Bernstorff , G. Jakopic and A. Haase, Vacuum **84**, 188 (2009).
[14]M. Ranjan, M. Bhatnagar and S. Mukherjee, J. App. Phy. **117**, 103106 (2015).
[15]R. Smith, Atomic and ion collisions in solids and at surfaces, Cambridge University Press, (2005).
[16]See supplemental material at for description of the interatomic potentials used to simulate the SiO_2 substrate and Ag-SiO_2 interaction.
[17]K. Jolley, R. Smith and K. Joseph, Nucl. Instr. Meth. B **352**, 140 (2015).
[18]T. Asano, T. N. Uetake and K. Suzuki, J. Nuc. Sci. and Tech. **29**, 1194 (1992).

[19] J. F. Groves, Directed vapor deposition, PhD Thesis, University of Virginia, (1998).
[20] K. L. Chopra, Thin Film Phenomena, McGraw-Hill, New York, (1969).
[21] C. Scott, S. Blackwell, L. Vernon, S. Kenny, M. Walls and R. Smith, J. Chem. Phys. **135**, 174706 (2011).
[22] G. Henkelman, B.P. Uberuaga and H. Jonnson, J. Chem. Phys. **113**, 9901 (2000).
[23] H. Wu and A. Anders, J. Phy. D: Appl. Phy. **43**, 065206 (2010).